Ultrafast Deformation of the Geometrical Structure of CO_2 Induced in Intense Laser Fields

Akiyoshi Hishikawa, Atsushi Iwamae, and Kaoru Yamanouchi*

Department of Chemistry, School of Science, University of Tokyo, 7-3-1 Hongo, Bunkyo-ku, Tokyo 113-0033, Japan

(Received 4 January 1999)

Ultrafast deformation of geometrical structure of CO_2 in an intense laser field (1.1 PW/cm^2 = 1.1 × 10^{15} W/cm^2) was investigated by momentum imaging of the fragment O^{p+} and C^{q+} ($p, q = 1-3$) ions produced from CO_2^{z+} through the Coulomb explosion processes, $CO_2^{z+} \rightarrow O^{p+} + C^{q+} + O^{r+}$ ($z = p + q + r$). The observed large mean amplitude along the ∠O—C—O bond angle (~40°) was attributed to the ultrafast bending motion induced on the light-dressed potential energy surfaces.

PACS numbers: 33.80.Rv, 33.80.Eh, 33.80.Wz

Along with the recent development of high-power short-pulsed lasers, ultrafast nuclear dynamics of molecules in an intense laser field [10^{-3}–1 PW/cm^2 (1 PW = 1 × 10^{15} W)] is becoming now one of the most fascinating subjects for deeper understanding of the light-matter interactions. Such nuclear dynamics has been studied intensively for H_2^+ whose large transition moment causes a strong laser-induced coupling between the bound $\sigma_g 1s$ and repulsive $\sigma_u 1s$ states. A new class of phenomena, e.g., the above-threshold dissociation, the bond softening, and the bond hardening, found in the molecular system has been best described in a dressed state picture, where a new adiabatic internuclear potential is formed through avoided crossings between molecular electronic states dressed by a photon field [1,2].

The formation of these new molecular potentials in an intense laser field can induce a drastic change in the geometrical structure of polyatomic molecules due to the nuclear motion on the light-dressed potential energy surfaces (LDPES). The laser-induced nuclear motion was investigated by Cornaggia *et al.* for CO_2 [3] on the basis of the distribution patterns in the covariance map of the fragment ions. It was argued that the covariance patterns between a pair of correlated fragment ions carry information of the geometrical structure of parent ions. On the other hand, the molecular structure just before the Coulomb explosion can be determined more directly from the spatial momentum vector distributions of the fragment ions, since they are sensitively dependent on the molecular geometry of the parent ion. In our recent studies, we developed a method to visualize the momentum vector distribution of mass selected fragment ions with respect to the polarization vector of the laser, called mass-resolved momentum imaging (MRMI), and it was successfully applied to diatomic molecules, N_2 [4,5] and NO [6], as well as to a polyatomic molecule, SO_2 [4]. In the present study, we apply this MRMI technique to CO_2 in an intense laser field (1.1 PW/cm^2) to determine the geometrical structure of multiply charged molecular ions, CO_2^{z+} ($z = 3-9$), from the momentum distribution of the fragment ions, O^{p+} ($p = 1-3$) and C^{q+} ($q = 1-3$), and follow quantitatively the structural deformation occurring in an ultrashort time scale both along the stretching coordinate and along the bending coordinate.

Details of our experimental setup have been described in the previous papers [4,5]. Briefly, the MRMI maps were constructed from the time-of-flight (TOF) spectra of the fragment ions recorded at 18 different angles of the polarization direction of the laser light with respect to the TOF detection axis. Figures 1(a) and 2(a) show the observed MRMI maps for all the fragment atomic ions, O^{p+} ($p = 1-3$) and C^{q+} ($q = 1-3$), produced after the (p, q, r) Coulomb explosion of CO_2, i.e., $CO_2^{z+} \rightarrow O^{p+} + C^{q+} + O^{r+}$, at the field intensity of 1.1 PW/cm^2 evaluated for the femtosecond laser light (100 fs, 795 nm, 0.74 mJ) focused to the beam diameter of 29 μm (the diffraction limit). The MRMI maps for the O^+, O^{2+}, and O^{3+} ions exhibit a pair of symmetrical crescentlike distributions located along the vertical axis with a symmetry center at the zero-momentum position. This means that these O^{p+} ions tend to be ejected in the laser polarization direction. Similar momentum distributions observed for diatomic molecules [4–6] exhibited some fine structures resulting from the overlapping of a few different pathways having a thinner crescentlike distribution. In the present case, a larger number of different pathways contributing to the O^{p+} channels overlap with each other, resulting in smooth and broad distributions. For example, the MRMI map for the O^{2+} ion is considered to be formed mainly from the six different fragmentation pathways having a fraction of more than 8%, i.e., $(p, q, r) = (2, 1, 1)$, $(2, 1, 2)$, $(2, 2, 1)$, $(2, 2, 2)$, $(2, 2, 3)$, and $(2, 3, 2)$. A thin crescent feature seen for the O^+ channel along the circle with a radius of ~100 × 10^3 amu m/s is assigned to the two-body fragmentation pathway, $CO_2^{2+} \rightarrow O^+ + CO^+$, on the basis of the MRMI map for the counterpart CO^+ ion.

The observed MRMI maps for C^{q+} ($q = 1-3$) are shown in Fig. 2(a). All the C^{q+} channels have an elliptical pattern substantially extending perpendicular to the laser polarization with a peak at the zero momentum. Figure 2(a) shows that these C^{q+} ions gain only small released momenta even though they are formed from the highly charged parent ions, and that they are ejected more

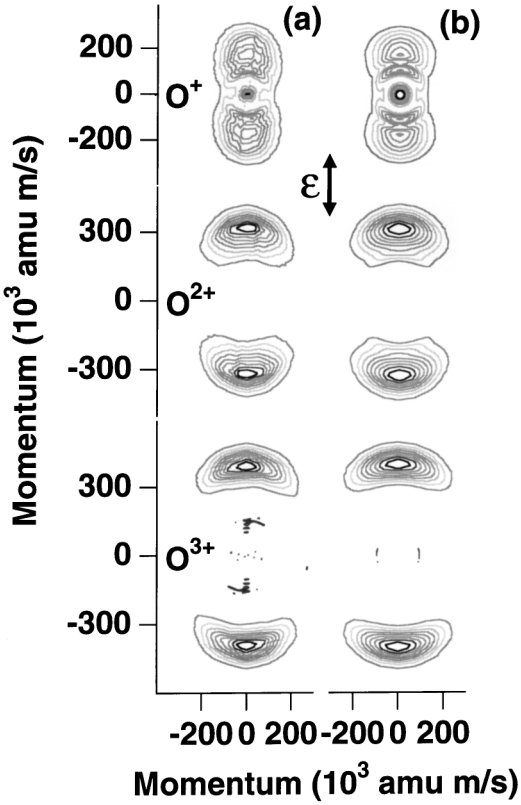

FIG. 1. The MRMI maps of the O^{p+} ($p = 1-3$) fragment ions produced through the Coulomb explosion of CO_2 in an intense laser field plotted against the polarization vector (ε) of the laser: (a) The observed results at the laser-field intensity of 1.1 PW/cm^2. (b) Best fit MRMI maps synthesized by the simulation. The simulated result for O^+ channel shows a clearer gap in the momentum region between the three- and two-body pathways, which is attributed to the small contribution from neutral pathways.

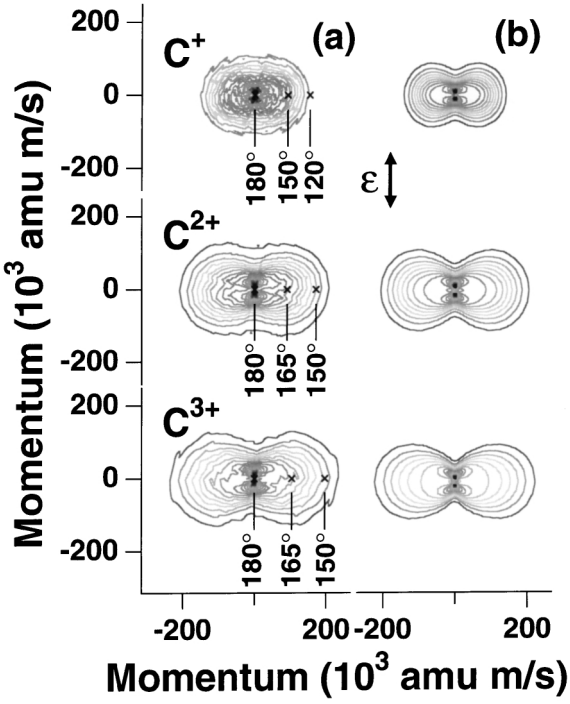

FIG. 2. The MRMI maps of the C^{q+} ($q = 1-3$) fragment ions: (a) The observed results. (b) The best fit MRMI maps obtained after the trial-and-error analysis.

preferentially in the direction perpendicular to the laser polarization vector.

From the observed MRMI maps of C^{q+} and O^{p+}, it can be inferred that the molecular a axes of the highly charged parent ions, CO_2^{z+} ($z = 3-9$), are aligned along the laser polarization vector, and that the average geometry is kept linear during the interaction with the intense laser field. A rough estimate of the geometry of CO_2^{z+} just before the explosion can be made directly from these MRMI maps. From the released momenta, 300×10^3 amu m/s for O^{2+} and 0 amu m/s for C^{2+}, the C—O bond length is calculated to be 2.5 Å. This is about twice as large as the equilibrium internuclear distance of neutral CO_2 ($R_e = 1.16$ Å) [7].

At the linear geometry, the centered C^{q+} ion is located at the unstable equilibrium position in the Coulomb field formed by the two adjacent O^{p+} and O^{r+} ions. Therefore, the momentum distributions for C^{q+} should be sensitively dependent on the bond angle of CO_2^{z+}. In Fig. 2, three selected points in the released momenta of each C^{q+} are converted to the bond angle $\gamma = \angle$O—C—O, where the most abundant symmetric fragmentation pathways, (1, 1, 1), (2, 2, 2), and (2, 3, 2), are assumed for C^+, C^{2+}, and C^{3+}, respectively. In the calculation, the $R = R$(C—O) values in Fig. 3 were adopted, which were determined from the analysis of the MRMI maps described below. Considering the mean amplitude of bending, $\sigma_\gamma = 12.5°$, in the ground vibrational level of the $\tilde{X}\,^1\Sigma_g^+$ state of neutral CO_2, the MRMI maps for C^{q+} clearly show that a substantially broad γ distribution centered at the linear configuration is induced in the intense laser field. The present observation is in agreement with the report by

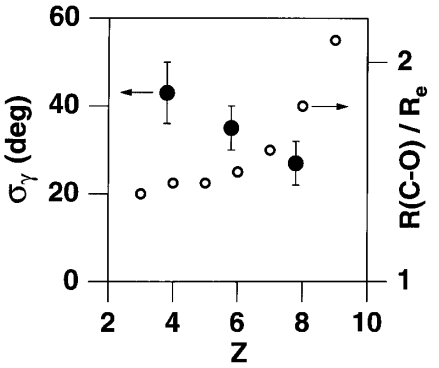

FIG. 3. The determined structural parameters R_0 (open circle) and σ_γ (solid circle) of CO_2^{z+} just before the Coulomb explosion as a function of z. Note that σ_γ is plotted against the weight-averaged charge number $\bar{z}$ of the parent ion (see text).

Cornaggia [7], who assumed a simple triangle distribution and derived its FWHM to be 40° for $z = 3$–6.

In order to derive more quantitative information concerning the structure of CO_2^{z+} prior to the dissociation, we performed a trial-and-error simulation of the MRMI maps of all the atomic fragment ions by taking the following steps: (i) the released momenta of fragment ions for a given molecular geometry are calculated, and they are converted into the MRMI maps for a single (p, q, r) explosion pathway, $CO_2^{z+} \rightarrow O^{p+} + C^{q+} + O^{r+}$, by taking account of the distributions of R and γ, (ii) the MRMI map for a given fragment ion is synthesized by adding the relevant single-pathway MRMI maps with their weights estimated from the observed yields of O^{p+}, and (iii) the geometrical parameters R and γ are determined on the basis of the trial-and-error comparison of the synthesized and observed MRMI maps for all the fragment ions.

The geometry of CO_2 ions just before the explosion is expressed in terms of the bond-angle distribution, $F_\gamma(\gamma) \propto \exp[-(\gamma - \pi)^2/(\sigma_\gamma/2\sqrt{\ln 2})^2]$, and the bond-length distribution, $F_R(R) \propto \exp[-\eta(1/\sqrt{R} - 1/\sqrt{R_0})^2]$, where σ_γ and R_0 are treated as adjustable parameters, while η is fixed to be 1.2×10^2 throughout the present study to give the same FWHM, ~1 Å, in the bond-length distribution as H_2 [8], N_2 [9], and NO [6] in the intense laser field (~1 PW/cm^2). We adopted the expression given by Friedrich and Herschbach [10] to describe the alignment of parent ions, $F_\theta(\theta) \propto \exp[-\sin^2\theta/(2\sigma_\theta^2)]$, where θ is the angle between the a axis and the laser polarization vector, and the distribution width, σ_θ, is treated as a parameter describing the alignment of parent ions caused both by the torque given to neutral CO_2 by the laser field [10] and by the ionization enhancement for a molecule having its molecular axis parallel to the polarization vector [11,12]. The above expression for $F_\theta(\theta)$ was found to reproduce well the angular distribution of the fragment ion produced through the Coulomb explosion of NO in an intense laser field [6]. For simplicity, σ_θ is approximated as a linear function of z in the present work. By numerically solving the classical equation of motion under the assumption that the repulsive forces between fragment ions are all Coulombic, the released momentum distribution $F(p_m, \theta_m^0)$ is calculated for the (p, q, r) fragmentation pathway with given $F_\gamma(\gamma)$ and $F_r(R)$, where p_m and θ_m^0 are the released momentum and the direction of the ion ejection in the molecule-fixed frame, respectively. Then, the MRMI maps for the single (p, q, r) explosion pathway are synthesized using the derived $F(p_m, \theta_m^0)$ as described previously [5].

The yields for respective (p, q, r) pathways were estimated in the following manner from the relative yields of the O^+, O^{2+}, and O^{3+} ions ejected in the solid angle of 4π, 1.0:1.9:0.40, obtained by integrating the MRMI maps [5,9] of these ions. It has been established from previous experimental studies for diatomic molecules that fragmentation pathways with a highly asymmetric charge separation, e.g., $N_2^{4+} \rightarrow N^{3+} + N^+$, are minor pathways [5,13]. Therefore, we assume that the fragmentation from a given charge state of the parent ion, $CO_2^{z+} \rightarrow O^{p+} + C^{q+} + O^{r+}$, that fulfills three inequalities, $|p - q| \leq 1$, $|q - r| \leq 1$, and $|r - p| \leq 1$, occurs with an equal probability. Based on these conditions, the relative yields of O^+, O^{2+}, and O^{3+} ions can be derived for a given charge distribution of CO_2^{z+} ($z = 0$–9). The charge distribution is expressed here by a Gaussian from an analogy of N_2 [5], where a smooth charge distribution was obtained. The mean z value at which the center of the Gaussian is located and its width are determined so that they reproduce the observed relative yields of the O^+, O^{2+}, and O^{3+} ions. This procedure in turn determines the relative yields of the respective fragmentation pathways. The derived yields showed that the contribution from the neutral pathways, in which at least one of the fragments has no charge, is less than 8% for O^+ and C^+ channels and is negligibly small for the higher charged fragments. Therefore, the neutral pathways are neglected in the analysis.

The geometrical parameters, σ_γ and R_0, as well as the alignment parameter σ_θ, were adjusted in a trial-and-error analysis until the observed MRMI maps for all the ion species, i.e., O^+, O^{2+}, O^{3+}, C^+, C^{2+}, and C^{3+}, are reproduced simultaneously. It was found that the momentum distributions of O^{p+} were much less sensitive to a small change in the Gaussian width σ_γ for the bond angle than those of C^{q+}. Therefore, a Gaussian width $\sigma_\gamma(q)$ describing the effective bond-angle distribution of CO_2^{z+} having a certain range of z is assigned to each C^{q+} channel. Using the determined relative yields of the fragmentation pathways, the weighted-average charge numbers $\bar{z}$'s of the parent ion are calculated to be $\bar{z} = 3.8$, 5.8, and 7.8, for C^+, C^{2+}, and C^{3+}, respectively. The determined structural parameters are shown in Fig. 3.

Figures 1(b) and 2(b) show, respectively, the best fit MRMI maps for O^{p+} ($p = 1$–3) and C^{q+} ($q = 1$–3) obtained after several iterations, reproducing well the observed MRMI maps. The alignment parameter is determined to be $\sigma_\theta = 0.375$–$0.025z$. The experimental values of σ_θ ranging from 0.30 to 0.15 for $z = 3$–9 are 5 to 2.5 times as large as a theoretical estimate of $\sigma_\theta = 0.06$ calculated using the formula proposed in Ref. [10] with the polarizability anisotropy and the rotational constant of CO_2, and the laser field intensity of 1.1 PW/cm^2. The discrepancy could be attributed to the incomplete formation of the pendular states within a short laser pulse, and/or to the saturation effect in the ionization process.

The bond length R(C—O) determined as a function of z exhibits a gradual increase as shown in Fig. 3, which is consistent with the recent studies of diatomic molecules, N_2 [9] and NO [6] in an intense laser field (~1 PW/cm^2). Previous theoretical [14,15] and experimental [11,16] studies show that the ionization rate of small molecules is substantially enhanced at an elongated molecular structure in an intense laser field, where the field ionization plays a

dominant role. We estimated the laser-field intensity necessary for the ionization as a function both of R and γ, by applying a classical field ionization model [16] for the ionization process of $CO_2^{2+} \rightarrow CO_2^{3+} + e^-$ as an example. It was found that the appearance intensity for CO_2^{3+}, calculated by fixing the molecular O—O axis in the direction parallel to the laser polarization, exhibited a pronounced minimum at the critical distance $R_c \sim 3.5R_e$ as seen in the case of N_2 calculated by Posthumus *et al.* [16]. This R dependence of the appearance intensity implies that each ionization step, $CO_2^{z+} \rightarrow CO_2^{(z+1)+} + e^-$, occurs at larger distance R ($<R_c$) for larger z, which explains qualitatively the observed charge-dependent bond elongation in Fig. 3. The present calculation shows that the appearance intensity for $\gamma = 90°$ is about 1.5 times higher than that for $\gamma = 180°$ in the entire range of $2.5 \leq R \leq 6.0$ Å. This suggests that the ionization occurs more efficiently at a linear configuration than at a bent configuration, which leads to a smaller σ_γ value for higher charged CO_2^{z+}. Although this behavior is consistent with the gradual decrease in σ_γ as a function of $\bar{z}$ (Fig. 3), the observed overall broadening in the γ distribution cannot be explained by the field ionization model.

As discussed for the ionization of atoms in intense laser fields [17], the population transfer from the ground state to excited states is important when the laser-field intensity is 1–100 TW/cm^2. The observed broad γ distributions would be ascribed to the laser-induced population transfer to an excited state having a bent equilibrium; i.e., the linear ground and the excited bent state are coupled strongly by the intense laser field to form a significant avoided crossing resulting in a pair of adiabatic LDPES's. It is expected that the potential barriers of the lower component of the resultant adiabatic LDPES's along the bond-angle coordinate would be lowered at a high field intensity to cause potential softening along the bond-angle coordinate, which causes the ultrafast nuclear motion toward the bent structure within a laser-pulse duration.

The Walsh diagram of CO_2 [18] suggests that an electronically excited state of CO_2^{z+} ($z = 0$–4) could have a bent equilibrium as far as the $6a_1$ molecular orbital having a strong bent character is occupied. One of such states would be the $\tilde{A}\,^1B_2(^1\Delta_u)$ state of neutral CO_2 [18], which is located 46 000 cm^{-1} above the ground electronic state, requiring four photons to form LDPES's for the present laser wavelength.

Regarding the bond-length distribution of the parent ion, the strong enhancement of the ionization process at the bond length of $\sim 2R_e$ could dominate over an effect originating from the formation of the adiabatic LDPES, so that the observed bond-length distribution is explained simply by the enhanced ionization model. On the other hand, the ionization rate may be only weakly dependent on the bond angle, which enables us to identify the signature of the formation of the LDPES in the bond-angle distribution.

The authors thank Dr. K. Hoshina and Dr. M. Kono for their valuable discussions and assistance in the experiment. The present work was supported by the CREST (Core Research for Evolutionary Science and Technology) fund from the Japan Science and Technology Corporation.

*Author to whom correspondence should be addressed.

[1] A. D. Bandrauk, *Molecules in Intense Laser Fields* (M. Dekker Publishing, New York, 1993).
[2] A. Giusti-Suzor, F. H. Mies, L. F. DiMauro, E. Charron, and B. Yang, J. Phys. B **28**, 309 (1995).
[3] C. Cornaggia, F. Salin, and C. Le Blanc, J. Phys. B **29**, L749 (1996).
[4] A. Hishikawa, A. Iwamae, K. Hoshina, M. Kono, and K. Yamanouchi, Chem. Phys. Lett. **282**, 283 (1998).
[5] A. Hishikawa, A. Iwamae, K. Hoshina, M. Kono, and K. Yamanouchi, Chem. Phys. **231**, 315 (1998).
[6] A. Iwamae, A. Hishikawa, and K. Yamanouchi (to be published).
[7] C. Cornaggia, Phys. Rev. A **54**, R2555 (1996).
[8] G. N. Gibson, M. Li, C. Guo, and J. Neira, Phys. Rev. Lett. **79**, 2022 (1997).
[9] A. Hishikawa, A. Iwamae, and K. Yamanouchi (unpublished).
[10] B. Friedrich and D. Herschbach, J. Phys. Chem. **99**, 15 686 (1995).
[11] E. Constant, H. Stapelfelt, and P. B. Corkum, Phys. Rev. Lett. **76**, 4140 (1996).
[12] J. H. Posthumus *et al.*, J. Phys. B **31**, L553 (1998).
[13] K. Codling *et al.*, J. Phys. B **24**, L593 (1991).
[14] A. D. Bandrauk and J. Ruel, Phys. Rev. A **59**, 2153 (1999).
[15] T. Seideman, M. Y. Ivanov, and P. B. Corkum, Phys. Rev. Lett. **75**, 2819 (1995).
[16] J. H. Posthumus, A. J. Giles, M. R. Thompson, and K. Codling, J. Phys. B **29**, 5811 (1996).
[17] R. R. Freeman *et al.*, Phys. Rev. Lett. **59**, 1092 (1987).
[18] J. W. Rabalais, J. M. McDonald, V. Scherr, and S. P. McGlynn, Chem. Rev. **71**, 73 (1971).